Influence of Ancillary Ligands on the Kinetics and the Thermodynamics of H_2 Addition to $IrXH_2(PR_3)_2$ (X = Cl, Br, I and R = H, Me): Comparison between Density Functional Theory and Perturbation Theory

E. Clot* and O. Eisenstein

LSDSMS UMR 5636, Université de Montpellier II, CC 014, 34 095 Montpellier cedex 5, France

Received: November 21, 1997; In Final Form: March 4, 1998

The electronic influence of ancillary ligands on the addition of H_2 to $IrXH_2(PR_3)_2$ (X = Cl, Br, I; R = H, Me) has been studied. The reaction enthalpy and the activation energy for the formation of a molecular dihydrogen complex have been computed. Results from ab initio MO perturbation theory (MP2) and density functional theory (B3LYP) are compared. The calculated geometries are in good agreement with the experimental results for $IrClH_2(P^tBu_2Me)_2$ and $IrIH_2(H_2)(P^iPr_3)_2$. The binding energy of H_2 is underestimated by B3LYP, while it is overestimated by MP2. The results are improved by modeling the phosphine with PMe_3 instead of PH_3. The reaction enthalpies and the activation energies are in excellent agreement with the experimental data and follow the experimental trend along the halide series. The transition state for the addition corresponds to the deformation of the unsaturated fragment $IrXH_2(PH_3)_2$ with almost no interaction with the incoming H_2 molecule. The trends for the activation and thermodynamic enthalpies among the halide series are rationalized in terms of π donor ability of the halides and variable strength of the trans influence of the hydride ligand.

I. Introduction

The addition of H_2 to a transition metal center to form a dihydrogen complex[1−4] is a prerequisite for further cleavage of the H−H bond. For this reason, a better understanding of the kinetic and thermodynamic aspects of H_2 addition to several unsaturated metal fragments may shed some light on catalytic processes.

Among all factors, the electronic influence of the ancillary ligands plays a central role in the M−H_2 binding process. This process is qualitatively described according to the Dewar−Chatt−Duncanson model.[5] A subtle balance between σ donation from H_2 to an empty d_σ orbital on the metal and π back-donation from a filled d_π metal orbital to the empty σ^* orbital of H_2 is required to achieve M−H_2 binding without cleaving the H−H bond. Both charge-transfer mechanisms are influenced by the electron donor and/or acceptor ability of the ancillary ligands. The net result is a lengthening of the H−H bond, which may eventually lead to bond cleavage.

Experimentally, the synthesis of molecular hydrogen complexes can be achieved in numerous ways. A simple route consists of the direct addition of free molecular dihydrogen to unsaturated metal species such as 16-electron ML_5 d^6 complexes.[3,4,6] Halide-containing d^6 pentacoordinated complexes have been often used because the π donation from the halide stabilizes the very reactive unsaturated ML_5 fragment.[7−13] The case of $IrXH_2L_2$ (X = Cl, Br, I; L = phosphine) has been particularly well-studied because with bulky phosphines the complex can be isolated.[8,9] In 1990, Jensen et al. prepared a neutral Ir(III) molecular hydrogen complex by reaction of this complex with free H_2 (see Scheme 1 where P stands for PR_3 and X for Cl, Br, or I).[11]

It was shown that in solution both **1** and **2** exist in equilibrium.[11,12,14,15] Temperature-dependent proton NMR studies allowed the determination of thermodynamic[14,15] as well as kinetic[15] parameters for this reaction. The influence of the solvent on the thermodynamics of the very same reaction has also been investigated.[16] The molecular dihydrogen complex **2** is generally more stable than the unsaturated fragment **1** by about 10 kcal·mol^{-1} (when very bulky phosphines were used, **2** was not observed[12]), and the stability decreases in the order I > Br > Cl. The activation enthalpies for the addition reaction follow the opposite trend: I < Br < Cl.

SCHEME 1

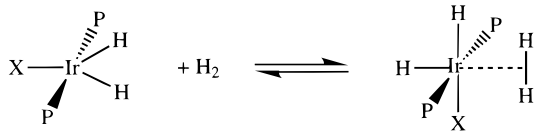

1 **2**

The theoretical description of such a reaction is challenging for several reasons. The binding energy of H_2 to the fragment is small and may therefore require considerable computational effort for proper representation. It is, for example, generally accepted that the Hartree−Fock (HF) approximation underestimates the M−H_2 interaction. For example, the use of PH_3 as a model for the phosphine ligand may introduce a systematic error because PH_3 does not have the electronic and/or the steric properties of the experimental bulky phosphines. Most often, however, PH_3 is used in the calculations with no clear understanding of the consequences of such simplification. A few studies have illustrated the importance of properly modeling the phosphine ligand.[17−19]

We have thus studied the addition of H_2 to $IrXH_2(PR_3)_2$ (X = Cl, Br, I and R = H, Me) with the purpose of computing the thermodynamic and kinetic parameters for this reaction. The calculations were done within the framework of ab initio MO perturbation theory (MP2) as well as with density functional

* Corresponding author. E-mail: clot@lsd.univ-montp2.fr.

S1089-5639(98)00284-9 CCC: $15.00
Published on Web 04/28/1998

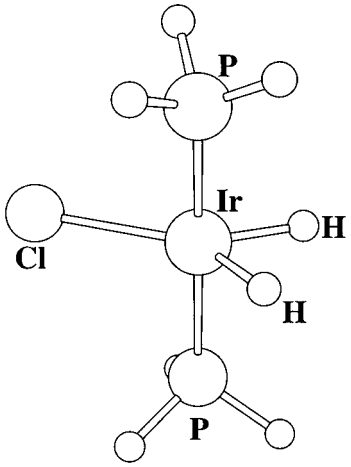

	Exp.	Calc.
Ir–Cl	2.410	2.42
Ir–P	2.325	2.304
Ir–H	1.553	1.548
H–Ir–H	72.7	69.

Figure 1. MP2-optimized geometry (distances in Å, angles in deg) of $IrClH_2(PH_3)_2$ and comparison with some geometrical parameters obtained for $IrClH_2(P^tBu_2Ph)_2$.[29]

theory (B3LYP), both of which are widely used for the study of transition metal complexes. The comparison of the results for the two methods will illustrate their respective ability to represent weakly bound systems. Moreover the variations in X and R should reveal the electronic influence of the halides on the reactivity. It should also give information on a proper modeling of the experimental phosphines.

II. Computational Details

All the calculations were performed with the Gaussian 94 set of programs.[20] Iridium was represented with the Hay−Wadt relativistic effective core potential (ECP) for the 60 innermost electrons and its associated double-ζ basis set.[21] The halides X (X = Cl, Br, I) and P were also described with Los Alamos ECPs and their associated double-ζ basis set[22] augmented by a polarization d function.[23] A 6-31G(p)[24] basis set was used for the hydrogen atoms bound to the metal. For the remaining hydrogen atoms (PH_3 and PMe_3) and the carbon atoms (PMe_3), a STO-3G basis set[25] was used.

Full geometry optimizations with no symmetry constraints have been carried out at three different levels. The Hartree−Fock approximation was found to be inadequate, and the results will not be reported unless needed. The ab initio MO perturbation theory (MP2 method[26]) and density functional theory (B3LYP) were selected for comparison. The exchange potential in B3LYP is the three-parameter hybrid functional of Becke,[27] and the correlation potential is that of Lee, Yang, and Parr.[28] In the case of $IrXH_n(PH_3)_2$ (X = Cl, Br, I and n = 2, 4), the nature of the stationary points was checked by numerical frequency calculations. For the PMe_3 case, only the updated Hessian was used to classify the stationary points, and the transition state for the reaction was not located.

III. Structure of the Unsaturated ML_5 Fragment

The geometry of $IrXH_2(PH_3)_2$ is a C_{2v} distorted trigonal bipyramid (Y-shaped) with an acute H−Ir−H angle and two axial phosphines. Figure 1 shows the MP2 geometry in the case of X = Cl where neutron diffraction results[29] are available ($IrH_2Cl(P^tBu_2Ph)_2$). Selected geometrical parameters are shown in Table 1 for the two methods. The calculated geometry is in good agreement with the experimental data with bond distances in general longer for B3LYP than for MP2.

The frequency calculations show these structures (X = Cl, Br, I and R = H) to be local minima for both methods. Table 2 shows the vibrational frequencies for modes involving the hydrides, and Scheme 2 illustrates the motions associated with these modes. The most intense band is the symmetric stretch around 2250 cm^{-1}, in excellent agreement with the band seen experimentally for $IrClH_2(PR_3)_2$[12] at 2232 cm^{-1} for R = Cy and at 2249 cm^{-1} for R = ^{i}Pr. Although the agreement is better with MP2, the values for B3LYP are very close. Note that the two methods do not give the same order for the M−H stretching modes. For MP2 the symmetric stretch has a lower frequency than the antisymmetric one, and the reverse order is found for B3LYP.

TABLE 1: Geometrical Parameters (Distances in Å, Angles in deg) for the $IrXH_2(PH_3)_2$ Ground State

	B3LYP			MP2		
	X = Cl	X = Br	X = I	X = Cl	X = Br	X = I
Ir−X	2.443	2.594	2.771	2.420	2.557	2.733
Ir−P	2.311	2.312	2.313	2.304	2.305	2.306
Ir−H	1.563	1.564	1.564	1.548	1.549	1.550
∠H−Ir−H	69.4	70.6	72.0	69.0	70.3	71.4

TABLE 2: Vibrational Frequencies (cm^{-1}) for the Bending and Stretching Modes of the Hydrides in $IrXH_2(PH_3)_2$ (X = Cl, Br, I)[a]

	B3LYP			MP2		
	X = Cl	X = Br	X = I	X = Cl	X = Br	X = I
bend AS	245	214	171	309	277	249
bend S	925	916	906	916	922	924
stretch S	2282	2276	2274	2242	2239	2236
stretch AS	2264	2254	2246	2310	2297	2283

[a] AS stands for antisymmetric and S for symmetric.

SCHEME 2

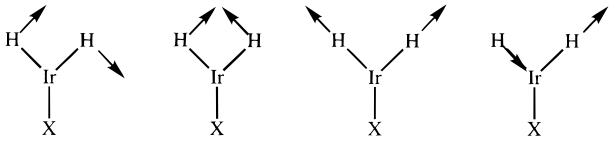

Despite this difference, both methods give an analogous trend along the halide series. The frequency of each mode decreases in the order Cl > Br > I with the exception of the symmetric bending mode with MP2. The variation of the antisymmetric bending mode is especially informative in terms of the role played by the halides. This bending mode (Scheme 2) is associated with the transformation of the distorted trigonal bipyramid Y into a square pyramid T. While there is π bonding between the metal and the halide in the Y-shaped structure, there is none in the T-shaped one.[13,30−32] An increase in the frequency of this mode is therefore indicative of stronger π bonding in the Y form, which stabilizes it relative to the T-shaped one in which the π bonding is partially or fully destroyed. The calculated frequencies therefore suggest that the π donating ability decreases from chlorine to bromine and iodine, in accord with the experimentally established trend.[33]

The unsaturated species needs to be distorted toward a T geometry to add H_2. The Y-shaped geometry of the complex is to be compared with two T-shaped structures that may add molecular H_2 (Scheme 3; the phosphines have been omitted for clarity). The T_X structure can be excluded because the combination of two strong σ donors (H) trans to each other, along with a poor σ donor (X) trans to a vacant site, gives a structure of very high energy. A calculation at the B3LYP level results in an optimized T_{Cl} structure lying 49 kcal·mol^{-1} above

SCHEME 3

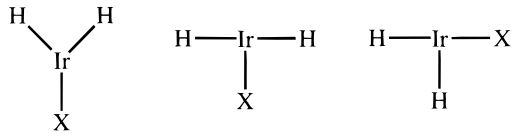

Y_X T_X T_H

TABLE 3: Geometrical Parameters (Distances in Å, Angles in deg) for the $IrXH_2(H_2)(PH_3)_2$ Ground State[a]

	B3LYP			MP2		
	X = Cl	X = Br	X = I	X = Cl	X = Br	X = I
Ir−X	2.534	2.686	2.861	2.506	2.644	2.813
Ir−P	2.316	2.319	2.320	2.306	2.308	2.310
Ir−H(1)	1.570	1.571	1.573	1.556	1.558	1.561
Ir−H(2)	1.590	1.590	1.591	1.571	1.573	1.576
Ir−H(3)	1.869	1.862	1.855	1.840	1.830	1.819
Ir−H(4)	1.883	1.876	1.863	1.859	1.849	1.836
H(3)−H(4)	0.810	0.813	0.819	0.808	0.813	0.821

[a] See Figure 2 for labeling of the hydrides.

the ground-state Y_{Cl} structure, with long Ir−H bond distances of 1.68 Å as a result of the strong mutual trans influence (see Table 1 for comparison with Ir−H distances in Y_{Cl}). In contrast, the chlorine, being trans to an empty site, moves closer to the metal (Ir−Cl = 2.36 Å).

Deformation toward T_H is energetically much easier,[29−32] because the strong σ donor ability of H favors its position trans to an empty site. Addition of H_2 is therefore kinetically favored with T_H compared to T_X. The bending modes of the hydrides suggest similar preferences for the regioselectivity of H_2 addition. The symmetric bending mode is stronger than the antisymmetric one (Table 2). This indicates that it is energetically more difficult to reach T_X than T_H. The lower antisymmetric bending mode permits the addition of H_2 trans to H as observed. From the relatively low value of the frequency, one can anticipate that the activation energy for H_2 addition will be small.

IV. Structure of the Molecular Hydrogen Complex

A. Comparison between the Methods. The geometry optimization of $IrXH_4(PH_3)_2$ (X = Cl, Br, I) results in a C_s molecular hydrogen complex where the H_2 lies in the molecular mirror plane containing the metal, X and both hydrides (Table 3). The frequency calculations confirmed these structures to be local minima. The MP2 geometry of $IrIH_2(H_2)(PH_3)_2$ is shown in Figure 2 as a representative of the whole family because a neutron diffraction structure for $IrIH_2(H_2)(PR_3)_2$ (R = ^{i}Pr) is available,[34] and it is therefore possible to compare the calculations directly with experimental results.

The bonding between Ir and X on one side, and the bonding between Ir and H_2 on the other are of particular importance and are especially poorly reproduced at the HF level. The M−H_2 binding energy is greatly underestimated, leading to an unreasonably short H−H distance (0.767 Å (HF) vs 0.856 Å (exptl)) and a long M−H_2 distance (1.93 Å vs 1.67 Å). The Ir−I distance is also not well-reproduced at this level (2.859 Å vs 2.770 Å). For the other bond distances (Ir−P and Ir−hydrides), the agreement is much better. For MP2 and B3LYP the theoretical Ir−I bond distances are too long. The best agreement is obtained with MP2 (2.813 Å vs 2.770 Å for the experimental value). The MP2 level accounts best here for both the saturated (Figure 2 and Table 3) and the unsaturated species (Figure 1 and Table 1).

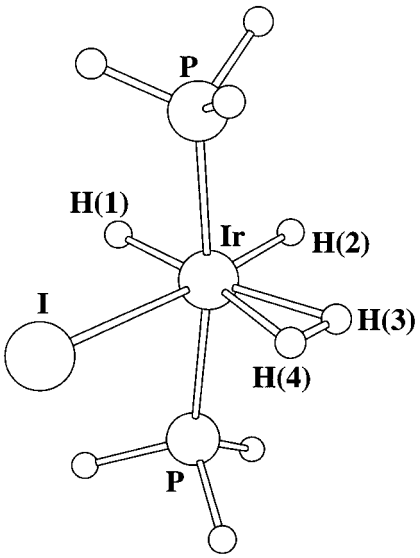

	Exp.	Calc.
Ir–I	2.770	2.813
Ir–P	2.336	2.310
Ir–H(1)	1.555	1.561
Ir–H(2)	1.577	1.576
Ir–H(3)	1.748	1.819
Ir–H(4)	1.764	1.836
H(3)–H(4)	0.856	0.821

Figure 2. MP2-optimized geometry (distances in Å, angles in deg) of $IrIH_2(H_2)(PH_3)_2$ and comparison with some geometrical parameters obtained for $IrIH_2(H_2)(PR_3)_2$ (R = ^{i}Pr).[34]

TABLE 4: Thermodynamic Values (kcal·mol^{-1}) for H_2 Addition to $IrXH_2(PH_3)_2$ (X = Cl, Br, I)[a]

	B3LYP			MP2			exptl		
	X = Cl	X = Br	X = I	X = Cl	X = Br	X = I	X = Cl	X = Br	X = I
ΔE	−3.5	−4.5	−5.8	−5.4	−6.6	−8.1			
ΔE + ZPE	−0.2	−0.7	−1.4	−1.3	−2.3	−3.9			
$\Delta_r H°$	−1.0	−2.0	−3.2	−2.9	−4.0	−5.7	−6.8	−7.9	−9.3

[a] The experimental values[15] refer to $IrXH_2(H_2)(P^tBu_2Me)_2$. See text for the definition of the energies.

To a first approximation, MP2 and B3LYP seem to give the same results with regard to the H_2 ligand. The H(3)−H(4) bond distances are almost identical, but differences appear in the Ir−H(3) and Ir−H(4) bond distances (Table 3). The H_2 ligand is closer to the metal, and the interaction between the metal and H_2 seems to be stronger with MP2 than with DFT. The energetics of the H_2 addition to the unsaturated fragment (Scheme 1) confirms this hypothesis. In Table 4 several ways to calculate the binding energy of H_2 to $IrXH_2(PH_3)_2$ (X = Cl, Br, I) are reported. The products are more stable than the reactants, and therefore these energy differences are negative. ΔE stands for the difference between the electronic energies. Frequency calculations allow computation of the zero-point energy (ZPE) and thermal enthalpy (T = 298.15 K and P = 1 atm). The reaction enthalpy $\Delta_r H°$ can then be calculated and compared with its experimental counterpart (Table 4). The energetics of the reaction are significantly influenced by inclusion of the vibrational effects. According to ΔE, the agreement between calculated and experimental values is very good (especially at the MP2 level). One might wrongly conclude that PH_3 correctly represents the electronic influence of the experimental phosphine (vide infra). In fact agreement is poorer with computed $\Delta_r H°$, especially for DFT. As already mentioned, the interaction between the metal and H_2 is stronger at the MP2 level compared to B3LYP. This underestimation by DFT may be attributed to the hybrid character of the exchange functional, as the Hartree−Fock approximation is poor for M−H_2 interaction, and so inclusion of HF exchange in B3LYP may be partly responsible for this failure.

To gain more insight into the relative behavior of the two methods, we computed the ΔE values at the CCSD(T) level[35]

TABLE 5: Electronic Energy Difference (kcal·mol^{-1}) ΔE for the Reaction in Scheme 1 at Different Post-Hartree−Fock Levels and with PH_3 as the Model Phosphine

	B3LYP	MP2	MP3	MP4D	MP4DQ	MP4SDQ	CCSD	CCSD(T)
X = Cl	−3.4	−5.4	−4.6	−4.5	−4.3	−4.5	−4.1	−4.4
X = Br	−4.4	−6.6	−5.4	−5.3	−5.1	−5.3	−4.8	−5.2
X = I	−5.6	−8.1	−6.6	−6.6	−6.4	−6.6	−6.0	−6.5

with the MP2 geometries. The objective was not to obtain better binding energies but to have a highly correlated result to compare with B3LYP and MP2. We also computed ΔE at the B3LYP level with the MP2 geometries to ensure consistency. Binding energies at these three levels as well as others are shown in Table 5. The average calculated binding energy (excluding B3LYP and MP2 from the average) for H_2 with PH_3 as a model phosphine is −4.4 kcal·mol^{-1} (X = Cl), −5.2 kcal·mol^{-1} (X = Br), and −6.4 kcal·mol^{-1} (X = I). B3LYP underestimates the M−H_2 interaction by 1 kcal·mol^{-1}, while MP2 overestimates it by about the same amount.

This difference in behavior may have great importance for the study of the oxidative addition of H_2. There are three domains for the binding of H_2 to a metal: the dihydrogen complex, the dihydride, and the stretched H_2 system. The dihydrogen complex corresponds to a situation where H_2 gives little electron density and also receives little through back-donation. A small underestimation or overestimation of the M−H_2 interaction may still give an H_2 complex as the preferred structure. For the dihydride case, each H acts as a strong σ donor and both methods are adequate to represent such an effect. Between these two domains (0.9 Å < H−H < 1.4 Å) lies the domain of stretched H_2 complexes.[36] The choice of the computational method is crucial for a proper representation of these last systems. Inaccuracies in computation of the M−H_2 interaction could result in a stretched H_2 complex falling into either the dihydrogen or dihydride domains. One can anticipate that MP2, overestimating the M−H_2 interaction, pushes the system toward completion of oxidative addition. On the other hand, B3LYP, underestimating the M−H_2 interaction, introduces a "delay" to the oxidative addition and yields molecular hydrogen complexes. A typical example of such a situation is $Ir(H_2)Cl_2H(PR_3)_2$ (R = ^{i}Pr), whose neutron structure has been determined.[29] The H−H bond distance (1.1 Å) classifies this complex as stretched or elongated. The calculated H−H bond distance at the MP2 level is 1.4 Å,[29] whereas the same model compound exhibits a H−H bond distance of 0.98 Å at the B3LYP level.[37] The use of a more sophisticated method results in better agreement as the H−H bond distance at the MCPF level[38] is 1.05 Å.[39] Thus, while dihydrogen complex and dihydride may be represented properly by the two methods, the intermediate region of bonding is much more difficult to describe, and bearing in mind the possible failure of DFT or MP2, more sophisticated methods should be used.

B. Influence of the Model Phosphine. The energies in Tables 4 and 5 clearly show that PH_3 is not a good model for phosphine. The binding energy of H_2 is underestimated and H(3)−H(4) bond distances (Table 3 and Figure 2) are too short for each method. The unsaturated fragments and the molecular hydrogen complexes were thus optimized with PMe_3 as a model phosphine (X = Cl, Br, I) at both B3LYP and MP2 levels.

The geometries with PMe_3 are very similar to those obtained with PH_3. Selected structural parameters are given in Tables 6 and 7. The general trend is toward an increase of all the bond distances. A closer inspection of the results for the unsaturated fragment (Table 6) reveals some differences between B3LYP and MP2. With B3LYP, replacing PH_3 by PMe_3 increases Ir−X and Ir−P bond distances by 0.035 and 0.04 Å, respectively,

TABLE 6: Geometrical Parameters for $IrXH_2(PMe_3)_2$ (Distances in Å, Angles in deg)

	B3LYP			MP2		
	X = Cl	X = Br	X = I	X = Cl	X = Br	X = I
Ir−X	2.483	2.634	2.813	2.447	2.582	2.755
Ir−P	2.343	2.345	2.349	2.326	2.328	2.331
Ir−H	1.560	1.560	1.560	1.544	1.545	1.545
∠H−Ir−H	71.1	72.6	74.0	70.3	71.7	73.1

TABLE 7: Geometrical Parameters (Distances in Å, Angles in deg) for $IrXH_2(H_2)(PMe_3)_2$[a]

	B3LYP			MP2		
	X = Cl	X = Br	X = I	X = Cl	X = Br	X = I
Ir−X	2.569	2.722	2.896	2.529	2.664	2.830
Ir−P	2.353	2.356	2.360	2.334	2.338	2.341
Ir−H(1)	1.575	1.575	1.578	1.566	1.567	1.571
Ir−H(2)	1.586	1.586	1.586	1.568	1.570	1.572
Ir−H(3)	1.830	1.828	1.822	1.773	1.769	1.762
Ir−H(4)	1.851	1.846	1.838	1.801	1.796	1.787
H(3)−H(4)	0.822	0.825	0.830	0.837	0.843	0.851

[a] See Figure 2 for labeling of the hydrides.

while the increase is approximately 0.025 Å for these two distances with MP2. Replacing PH_3 with the more basic PMe_3 clearly induces a greater elongation of metal ligand bonds for the B3LYP method than for MP2. Nonetheless, the geometry obtained for $IrClH_2(PMe_3)_2$ with MP2 is in very good agreement with the experimental structure (Figure 1 and Table 6).

The same difference between MP2 and B3LYP is obtained for the molecular hydrogen complex upon replacement of PH_3 by PMe_3 (Table 7). The increase in Ir−X and Ir−P bond distances is 0.04 Å for B3LYP (0.025 for MP2). The Ir−I bond distance is poorly represented by B3LYP (2.896 vs 2.770 Å experimentally), and the H_2 ligand is still too far from the metal (Table 7 and Figure 2). MP2 does not improve the description of the Ir−I bond, still yielding an unreasonably long distance (2.830 Å), but the geometry of the coordinated H_2 ligand is excellent. Not only is the H(3)−H(4) distance very close to experiment (0.851 vs 0.857 Å exptl) but the Ir−H(3) and Ir−H(4) bonds are significantly improved compared to the PH_3 case (Tables 3 and 7) and are in excellent agreement with experiment. Moreover the Ir−P bond distance with MP2 closely matches the experimental one (2.341 Å calcd vs 2.336 Å exptl). The MP2 level of theory with PMe_3 as a model phosphine thus gives a fairly accurate description of the experimental complexes. For this particular system, B3LYP results in a poorer although still fair description of the experimental complexes.

It is not only the structure that is improved by replacing PH_3 with PMe_3 but also the energetics. In Table 8 the ΔE values (electronic energy difference between the reactants and the products) are reported for the case of PMe_3. They were also calculated at the MP4 level (with MP2 geometries) to provide a better estimate of the binding energy. The experimental $\Delta_r H°$ values are reported for comparison. H_2 is bonded more strongly with PMe_3 than with PH_3. The energy gain is around 1.5 kcal·mol^{-1} for B3LYP and 2.0 kcal·mol^{-1} for MP2 (Tables 4 and 8). Thus the change of phosphine has not altered the general behavior of the two methods. Binding energies are still lower with B3LYP than with MP2. Furthermore the increase of

TABLE 8: Electronic Energy Difference (kcal·mol^{-1}) ΔE for the Reaction in Scheme 1 at Different Post-Hartree−Fock Levels and with PMe_3 as a Model Phosphine[a]

	B3LYP	MP2	MP4	exptl
X = Cl	−5.1	−7.8	−7.2	−6.8
X = Br	−6.0	−8.8	−8.1	−7.9
X = I	−7.2	−10.2	−10.2	−9.3

[a] The experimental values[15] concern the compound $IrXH_2(H_2)(P^tBu_2Me)_2$.

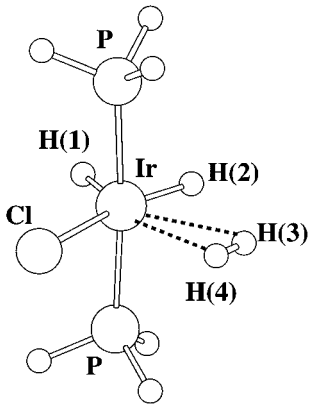

Figure 3. MP2-optimized geometry (distances in Å, angles in deg) of the transition state corresponding to H_2 addition to $IrClH_2(PH_3)_2$.

M−H_2 binding energy upon replacement of PH_3 by PMe_3 is even larger with MP2, which magnifies the difference between the two methods.

By subtracting the appropriate numbers in Table 4 (PH_3), one notices that the difference between computed ΔE and $\Delta_r H°$ values is the same for each method and each halide, namely, 2.5 kcal·mol^{-1}. Assuming the same energy shift for the PMe_3 case, the estimated $\Delta_r H°$ values at the MP2 level are −5.3 kcal·mol^{-1} (X = Cl), −6.3 kcal·mol^{-1} (X = Br), and −7.7 kcal·mol^{-1} (X = I). Thus experimental and theoretical results differ by no more than 1.5 kcal·mol^{-1}, which is remarkable considering the size of the basis set and the level of theory. The use of PMe_3 as a ligand improves the results significantly. PH_3 is clearly not basic enough to correctly model the experimental phosphines; when the electron density at the metal center is a key issue, this may have dramatic consequences.

V. Structure of the Transition State

The small M−H_2 binding energies are accompanied by very small activation energies for the addition reaction, which have been determined by ^{1}H NMR for the three halides ($\Delta_r H^‡ < 3$ kcal·mol^{-1}). This suggests that the M−H_2 interaction in the transition state should be very small and thus, in particular, the H−H distance is hardly elongated from the equilibrium value for free H_2. The transition state for H_2 addition to $IrXH_2(PH_3)_2$ (X = Cl, Br, I) was located at the B3LYP and MP2 levels. The initial guess for the geometry of the transition state was a dihydrogen molecule coplanar with Ir−X and distant from the metal fragment (in the Y geometry) by 3 Å. Frequency calculations have confirmed its nature as a transition state. As a typical example of the results, the MP2-optimized geometry for X = Cl is represented in Figure 3, and geometrical parameters for the whole series are reported in Table 9.

The computed activation parameters are reported in Table 10. The agreement with experiment is excellent especially with MP2. Inclusion of the vibrational effects here also improves the values. The main result is the absence of significant

TABLE 9: Geometrical Parameters (Distances in Å, Angles in deg) for the Transition State Corresponding to H_2 Addition to $IrXH_2(PH_3)_2$[a]

	B3LYP			MP2		
	X = Cl	X = Br	X = I	X = Cl	X = Br	X = I
Ir−X	2.489	2.637	2.805	2.465	2.599	2.769
Ir−P	2.312	2.314	2.315	2.304	2.305	2.307
Ir−H(1)	1.542	1.542	1.543	1.530	1.531	1.531
Ir−H(2)	1.583	1.583	1.584	1.563	1.565	1.569
Ir−H(3)	2.751	2.808	2.763	2.680	2.680	2.550
Ir−H(4)	2.762	2.821	2.955	2.758	2.852	2.974
H(3)−H(4)	0.747	0.747	0.747	0.738	0.738	0.740

[a] See Figure 3 for labeling of the hydrides.

interaction between the metal and H_2 in the transition state. This now explains why MP2 and B3LYP give very similar results since these methods differ mostly in their estimate of the M−H_2 interaction.

The geometry of the transition state corresponds to a reactant-like structure slightly distorted by a very weakly bound H_2 ligand (Table 9). The H−H bond distance is identical to that of free H_2. The ML_5 fragment is distorted to create more space for the incoming H_2. The transition state is thus an early transition state with respect to every geometrical parameter, and the activation energy is mostly used to distort the ML_5 fragment.

From the geometrical parameters there seems to be no interaction between the metal and H_2 in the transition state. To investigate this observation more closely, the energy of the transition-state structure without the H_2 ligand (structure TS_H_2) was calculated and compared to that of Y_X. For complete comparison, we have also added (Table 11) the energies of the product deprived of the H_2 ligand (prod_H_2). The energies (ΔE values) of the transition state (Table 10) and of the structure TS_H_2 (Table 11) relative to their respective Y origin are very close, especially at the B3LYP level. This confirms that, at this level, there is essentially no interaction in the transition state between the metal and H_2. At the MP2 level, the M−H_2 interaction is slightly stronger (0.5 kcal·mol^{-1}) and the activation energy to reach the TS is slightly lower than that to distort the reactant. This illustrates once more that there is more M−H_2 interaction with MP2 than with B3LYP.

The deformation of the unsaturated fragment to form the transition state involves the disruption of the π interaction between the metal and the halide. It is thus more energetically difficult to reach the transition state for a stronger Ir−X π bond (Cl > Br > I). This trend agrees with the experimental results of Caulton.[33]

In addition to weakening the Ir−X π bond, the Y-to-T-shaped distortion results in a change in the metal−ligand σ bonds. In the T structure, one hydride and the halide are trans to each other. Keeping in mind that a hydride has a strong σ influence, it is more favorable to position an iodide trans to H than a chloride because I is more polarizable and is thus able to adapt more easily to the bonding requirement of the hydride. In other words, the energy cost associated with the Y-to-T transformation increases in the order I < Br < Cl. Thus in the transition state the H(2)−Ir−X angle (MP2) decreases in the same order (I, 166.8° > Br, 164.7° > Cl, 164.3°) in order to minimize this destabilization.

It is worth noting that H(2)−Ir−X varies in the opposite way in the final product (I, 173° < Br, 173.8° < Cl, 174.7°). Even though such differences are very small, they are indicative of the developing stabilizing Ir−H_2 interaction. A stronger Ir−H_2 interaction requires higher electron density at the metal to maximize the back-donation into $\sigma^*_{H_2}$. Setting two ligands

TABLE 10: Activation Parameters (kcal·mol^{-1}) for H_2 Addition to $IrXH_2(PH_3)_2$ (X = Cl, Br, I)[a]

	B3LYP			MP2			exptl		
	X = Cl	X = Br	X = I	X = Cl	X = Br	X = I	X = Cl	X = Br	X = I
ΔE	+2.3	+2.1	+1.7	+1.9	+1.8	+1.4			
ΔE + ZPE	+3.7	+3.3	+2.7	+3.2	+2.9	+2.6			
$\Delta_r H^{\ddagger}$	+2.9	+2.6	+1.6	+2.5	+2.3	+1.9	+2.6	+2.3	+2.0

[a] The experimental values[15] concern the compound $IrXH_2(H_2)(P^tBu_2Me)_2$.

TABLE 11: Relative Energy (kcal·mol^{-1}) of Various ML_5 Fragments Involved in the Process of H_2 Addition to $IrXH_2(PH_3)_2$ (X = Cl, Br, I) at the B3LYP and MP2 Levels[a]

	B3LYP			MP2		
	X = Cl	X = Br	X = I	X = Cl	X = Br	X = I
TS_H_2	+2.3	+2.	+1.6	+2.5	+2.2	+2.1
prod_H_2	+7.0	+6.4	+5.8	+8.9	+8.2	+7.5

[a] See text for definition of TS-H_2 and prod-H_2. Energies are in kcal·mol^{-1}.

with strong trans influence trans to each other accumulates more density at the metal, which results in a more basic metal fragment. Iodine, being less electronegative than chlorine, donates more electrons to the metal and thus does not need to be strictly trans to the hydride for the metal fragment to achieve an efficient Ir−H_2 interaction.

The subtle balance of metal−ligand interactions involved in the transition state and in the products during the addition of H_2 to $IrH_2X(PR_3)_2$ illustrates the difficulty of predicting the effect of ligands. It also suggests that changes in the magnitude of metal−ligand π interactions cannot be the sole factor involved in determining the reactivity of these 16-electron complexes.

Conclusions

In this work we have computed the thermodynamic and kinetic enthalpies for the addition of H_2 to $IrXH_2(PR_3)_2$ (X = Cl, Br, I; R = H, Me). The calculations have been done at the two most widely used levels of theory for this kind of inorganic systems: B3LYP and MP2. As the binding energy of H_2 to a transition metal to form a molecular hydrogen complex is rather small, the comparison between the two methods on this particular system was a test of their relative performance on weakly bound complexes.

As a general trend, MP2 tends to overestimate the interaction between H_2 and the metal while B3LYP underestimates it. Therefore, for systems that are on the borderline between the weakly bound and the strongly bound domains (stretched H_2 complexes for example), changing the method may have dramatic consequences. MP2, which overestimates the interaction, might push the system to the strongly bound domain (dihydride), while B3LYP tends to pull the system to the weakly bound domain (dihydrogen) by underestimating the interaction.

We have also shown that, for each method of calculation, the use of PMe_3 in place of PH_3 as a model phosphine significantly improves the structural and energetical results. The results with MP2 are thus very good. PH_3 is not a sufficiently strong electron donor to correctly simulate the electronic influence of the experimental phosphine. When the electronic density at the metal is a key issue, as for the H_2 binding process where a subtle balance between σ donation and π back-donation occurs, a proper representation of the phosphine is of critical importance.

Finally the experimental trends for the reaction and activation enthalpies are very well-reproduced (especially with MP2), and this trend can be explained in terms of π donor ability of the halide and the variable strength of the trans influence of the hydrides.

Acknowledgment. These calculations were carried out in part at the National CNRS computer facilities IDRIS. We are grateful to Dr. J. E. McGrady for helpful discussion.

References and Notes

(1) Kubas, G. J. *Acc. Chem. Res.* **1988**, *21*, 120.
(2) Crabtree, R. H. *Acc. Chem. Res.* **1990**, *23*, 95.
(3) Jessop, P. G.; Morris, R. H. *Coord. Chem. Rev.* **1992**, *121*, 155.
(4) Heinekey, D. M.; Oldham Jr., W. J. *Chem. Rev.* **1993**, *93*, 913.
(5) Crabtree, R. H., *The organometallic chemistry of the transition metals*; John Wiley & Sons: New York, 1988.
(6) Kubas, G. J.; Ryan, R. R.; Swanson, B. I.; Vergamini, P.; Wasserman, H. J. *J. Am. Chem. Soc.* **1984**, *106*, 451.
(7) Esteruelas, M. A.; Sola, E.; Oro, L. A.; Meyer, O.; Werner, H. *Angew. Chem., Int. Ed. Engl.* **1988**, *27*, 1563.
(8) Gusev, D. G.; Bakhmutov, V. I.; Grushin, V. V.; Volpin, M. E. *Inorg. Chim. Acta* **1990**, *175*, 19.
(9) Gusev, D. G.; Bakhmutov, V. I.; Grushin, V. V.; Volpin, M. E. *Inorg. Chim. Acta* **1990**, *177*, 115.
(10) Mezzetti, A.; Delzotto, A.; Rigo, P.; Farnetti, E. *J. Chem. Soc., Dalton Trans.* **1991**, 1525.
(11) Mediati, M.; Tachibana, G. N.; Jensen, C. M. *Inorg. Chem.* **1990**, *29*, 3.
(12) Mediati, M.; Tachibana, G. N.; Jensen, C. M. *Inorg. Chem.* **1992**, *31*, 1827.
(13) Caulton, K. G. *New. J. Chem.* **1994**, *18*, 25.
(14) Husebo, T. L.; Jensen, C. M. *Inorg. Chem.* **1993**, *32*, 3797.
(15) Hauger, B. E.; Gusev, D. G.; Caulton, K. G. *J. Am. Chem. Soc.* **1994**, *116*, 208.
(16) Lee, D. W.; Jensen, C. M. *J. Am. Chem. Soc.* **1996**, *118*, 8749.
(17) Lin, Z.; Hall, M. B. *J. Am. Chem. Soc.* **1992**, *114*, 2928.
(18) Matsubara, T.; Maseras, F.; Koga, N.; Morokuma, K. *J. Phys. Chem.* **1996**, *100*, 2573.
(19) Jacobsen, H.; Berke, H. *Chem. Eur. J.* **1997**, *3*, 881.
(20) Frisch, M. J.; Trucks, G. W.; Schlegel, H. B.; Gill, P. M. W.; Johnson, B. G.; Robb, M. A.; Cheeseman, J. R.; Keith, T.; Petersson, G. A.; Montgomery, J. A.; Raghavachari, K.; Al-Laham, M. A.; Zakrzewski, V. G.; Ortiz, J. V.; Foresman, J. B.; Peng, C. Y.; Ayala, P. Y.; Chen, W.; Wong, M. W.; Andres, J. L.; Replogle, E. S.; Gomperts, R.; Martin, R. L.; Fox, D. J.; Binkley, J. S.; Defrees, D. J.; Baker, J.; Stewart, J. P.; Head-Gordon, M.; Gonzalez, C.; Pople, J. A. *Gaussian 94*, Revision B.3; Gaussian Inc.: Pittsburgh, PA, 1994.
(21) Hay, P. J.; Wadt, W. R. *J. Chem. Phys.* **1985**, *82*, 299.
(22) Wadt, W. R.; Hay, P. J. *J. Chem. Phys.* **1985**, *82*, 284.
(23) Höllwarth, A.; Böhme, M.; Dapprich, S.; Ehlers, A. W.; Gobbi, A.; Jonas, V.; Köhler, K.; Stegmann, R.; Veldkamp, A.; Frenking, G. *Chem. Phys. Lett.* **1993**, *208*, 237.
(24) Harihan, P. C.; Pople, J. *Theor. Chim. Acta* **1973**, *28*, 213.
(25) Hehre, W. J.; Stewart, R. F.; Pople, J. A. *J. Chem. Phys.* **1969**, *51*, 2657.
(26) Møller, C.; Plesset, M. S. *Phys. Rev.* **1934**, *46*, 618.
(27) Becke, A. D. *J. Chem. Phys.* **1993**, *98*, 5648.
(28) Lee, C.; Yang, W.; Parr, R. G. *Phys. Rev. B* **1988**, *B37*, 785.
(29) Albinati, A.; Bakhmutov, V. I.; Caulton, K. G.; Clot, E.; Eckert, J.; Grushin, O. E. V. V.; Hauger, B. E.; Klooster, W. T.; Koetzle, T. F.; McMullan, R. K.; O'Loughlin, T. J.; Pélissier, M.; Ricci, J. S.; Sigalas, M. P.; Vymenits, A. B. *J. Am. Chem. Soc.* **1993**, *115*, 7300.
(30) Jean, Y.; Eisenstein, O. *Polyhedron* **1988**, *7*, 405.
(31) Rachidi, I. E. I.; Eisenstein, O.; Jean, Y. *New J. Chem.* **1990**, *14*, 671.
(32) Riehl, J. F.; Jean, Y.; Eisenstein, O.; Pélissier, M. *Organometallics* **1992**, *11*, 729.

(33) Poulton, J. T.; Folting, K.; Streib, W. E.; Caulton, K. G. *Inorg. Chem.* **1992**, *31*, 3190.
(34) Eckert, J.; Jensen, C. M.; Koetzle, T.; Husebo, T. L.; Nicol, J.; Wu, P. *J. Am. Chem. Soc.* **1995**, *117*, 7271.
(35) Pople, J. A.; Head-Gordon, M.; Raghavachari, K. *Chem. Phys. Lett.* **1987**, *87*, 5968.
(36) Michos, D.; Luo, X. L.; Howard, J. A. K.; Crabtree, R. H. *Inorg. Chem.* **1992**, *31*, 3914.
(37) Maseras, F.; Lledós, A.; Costas, M.; Poblet, J. M. *Organometallics* **1996**, *15*, 2947.
(38) Chong, D. P.; Langhoff, S. R. *J. Chem. Phys.* **1986**, *84*, 5606.
(39) Clot, E. Unpublished result.